

Atomistic calculations of defects in ZnGeP₂

Peter Zapol and Ravindra Pandey^{a)}

Department of Physics, Michigan Technological University, Houghton, Michigan 49931

Mel Ohmer

Wright Laboratory, Wright-Patterson Air Force Base, Ohio 45433

Julian Gale

Department of Chemistry, Imperial College of Science, Technology and Medicine, South Kensington, SW7 2AY London, United Kingdom

(Received 5 June 1995; accepted for publication 3 October 1995)

Atomistic calculations are performed to study defect energetics in ZnGeP₂ where two- and three-body interatomic potentials are used to simulate the perfect lattice. Formation energies for native ionic defects and binding energies for some of the electronic defect complexes are calculated. The dominance of antisite defect pairs, Zn_{Ge} + Ge_{Zn}, is predicted in the lattice. However, the defects controlling the spectroscopic properties would seem to be associated with vacancies. For the EPR-active acceptor center, the hole is found to be localized near the zinc vacancy rather than near the zinc antisite (Zn_{Ge}). The calculated results suggest that the reported Hall effect and the photoluminescence data are compatible with the existence of two acceptors in the lattice (in a three level model) where one is significantly shallower, experimentally by 0.27 eV, in reasonable agreement with the calculated difference of 0.37 eV. © 1996 American Institute of Physics. [S0021-8979(96)04302-3]

I. INTRODUCTION

Ternary chalcopyrite semiconductors are known to have large nonlinear optical coefficients making them candidates for second harmonic generation and optical parametric oscillator applications.¹⁻³ In this group, zinc germanium phosphide (ZnGeP₂) is one of the most promising members and has been proposed for 2.05 μm pumped type I oscillators.⁴⁻⁶ However, the presence of an absorption band near the pump wavelength limits the effectiveness of this material for device applications. This absorption band in the spectral region of 1–2 μm has been attributed to photoionization of a highly compensated deep native acceptor center (referred to as AL1).⁷⁻¹⁰ The acceptor is attributed to a zinc vacancy and its binding energy (E_v) is given as 0.4–0.6 eV. It is suggested that the compensating donor is a phosphorus vacancy. There is no indication in the literature of its binding energy since it cannot be easily determined as all bulk crystals are semi-insulating *p*-type crystals. In an analogous way, it should be a deep donor since in CdSiP₂ the P vacancy donor binding energy (E_c) has been given as 0.63 eV⁸ and the P vacancy donor in GaP, the binary analog of ZnGeP₂, is estimated as 0.3 eV.⁹ The concentration of both acceptors⁹ and donors⁷ has been typically in the range of 10¹⁹ cm⁻³.

The EPR studies on as-grown ZnGeP₂ have observed an acceptor center in the lattice with concentrations exceeding 10¹⁹ cm⁻³. This EPR-active center (related to the AL1 center) is considered to be associated with the native defect complex involving either a zinc vacancy (V_{Zn}) or a zinc ion on a germanium site (Zn_{Ge}).¹¹ A recent ENDOR study favors the singly ionized zinc-vacancy model.¹² In addition, a photoinduced EPR¹³ study indicates that the P vacancy is the dominant donor in this highly compensated material. Thus,

the experimental work on defect identification provides support for the traditional model described in the previous paragraph.

Theoretical studies on this material have been limited to perfect lattice only. The results of electronic structure calculations based on density functional theory were compared to x-ray photoemission spectra.¹⁴ A successful attempt has also been made to perform lattice dynamics calculations within the framework of rigid ion model.¹⁵ However, none of the theoretical efforts have been directed to understand the properties of defects in this material. In this article, we make such an attempt to perform a study on defective ZnGeP₂ using atomistic simulation techniques based on the shell model. We will first calculate the energies of Frenkel, Schottky, and antisite disorder in the lattice and will simulate the EPR-active acceptor center to provide the microscopic description for its identification. We note here that the shell model calculations have been shown as a highly effective tool for prediction of defect energetics in ionic and semi-ionic materials including sixfold- and fourfold-coordinated structures.^{16,17}

In Sec. II, we briefly describe the shell model obtaining the potential parameters fitted to the perfect lattice properties of the ZnGeP₂. The energetics and structure of ionic and electronic defects are discussed in Sec. III. The results are summarized in Sec. IV.

II. PERFECT LATTICE

We begin with the pair-potential description of the perfect lattice consisting of the shell-model ions. The two-body interatomic potential energy is then the sum of the long-range Coulombic and the short-range non-Coulombic contributions. We use a simple analytical expression of the Buckingham type for the short-range interaction between ions *i* and *j*:

^{a)}Electronic mail: pandey@phy.mtu.edu

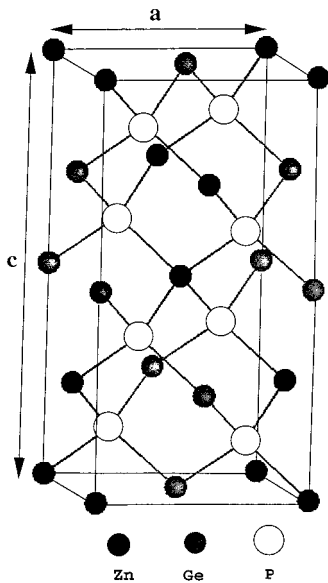


FIG. 1. Crystal structure of ZnGeP_2 .

$$V_{ij} = A \exp(-r_{ij}/\rho) - Cr_{ij}^{-6}, \quad (1)$$

where the term in r^{-6} is referred to as the dispersive term.

In the shell model,¹⁸ each point ion consists of a core of charge X , and a shell of charge Y , such that the total charge is the sum of the core and shell charges. The polarization of a shell-model ion is then described by the displacement of a shell from a core, the two being connected by a harmonic spring with a force constant K .

Potential parameters, both in the analytical representation of short-range interactions (A , ρ , and C) and in the shell-model treatment of ionic polarization (Y and K) are obtained by empirical fitting to the crystal structure¹⁹ and known elastic and dielectric constants.²⁰ The fractional coordinate of the P shell was also taken as a parameter because the location of the shell in the lattice is unknown.²¹ Fitting and all calculations were performed using the program GULP.²²

ZnGeP_2 crystallizes in the chalcopyrite phase with a symmetry space group of D_{2h}^{12} . The chalcopyrite phase can be considered as a superlattice of the cubic zinc blende with the $c/a=2$.¹ It can easily be obtained by replacing each half of cations by Zn and Ge ions, respectively, and introducing slight distortion (i.e., $c/a=1.958$) along z axis in the zinc-blende phase (see, Fig. 1). The tetrahedral coordination in the ZnGeP_2 lattice suggests that the covalent bonding (with sp^3

hybrid bonds) predominates. On the other hand, the composition of the cation sublattice (consisting of Zn and Ge) indicates a significant presence of the ionic character in the bonding.

Realizing this, we therefore do not begin with a fully ionic model assuming Zn^{2+} , Ge^{4+} , and P^{3-} ions, rather we fit the charges of the constituting ions to experimentally measured crystal constants.¹⁹ In this way, covalency is taken into account by use of the empirical fitting method which yields the fractional charges of +1.2 for Zn, +1.8 for Ge, and -1.5 for P. A similar use of fractional charges was proposed in the lattice dynamics calculations of ZnGeP_2 .¹⁵

In addition, three-body potentials were used for more accurate treatment of the many-body effects. They were taken in the Axilrod-Teller form,²³ which is derived from third-order perturbation theory as a triple-dipole interaction:

$$V_{ijk} = k_{ijk}(1 + 3 \cos \theta_i \cos \theta_j + \cos \theta_k)/R_i^3 R_j^3 R_k^3, \quad (2)$$

where k_{ijk} is a coefficient, θ_i and R_i are i th angle and side of the triangle formed by ions i , j , and k .

Table I lists the potential parameters representing the interatomic interactions in the lattice. In this potential model, we neglect the cation-cation short-range interactions and treat the Zn and Ge ions as rigid ions in the lattice. The calculated lattice properties are compared with the experimental data in Table II. Accordingly, the potential model reproduces the lattice structure very well. The overall good agreement between the calculated and experimental properties for the perfect lattice provides us with a sound basis for extending the model to defect calculations. In the absence of experimental data for elastic constants, we take guidance from the lattice dynamics calculations where a phenomenological rigid ion model with partial ionic charges was used to reproduce the vibrational spectrum of ZnGeP_2 .²⁴

III. DEFECTS

Defect energies of several plausible types of ionic and electronic defects have been calculated using the Mott-Littleton methodology.²⁵ Here, the lattice containing a defect is divided into two regions. Atoms in the inner region (immediately surrounding the defect) are treated explicitly and allowed to relax during the minimization procedure. The response of the outer region is obtained using macroscopic dielectric theory. In the present calculations the inner region consists of ~ 150 atoms. An increase of this region size in-

TABLE I. Two- and three-body short-range interaction and shell-model parameters for ZnGeP_2 . The charges on ions are taken to be $-1.5e$, $1.2e$, and $1.8e$ for P, Zn, and Ge, respectively.

	A (eV)	ρ (Å)	k (eV Å ⁻⁹)	Y (e)	K (eV Å ⁻²)
$\text{Ge}_c\text{-P}_s$	328.03	0.3937			
$\text{Zn}_c\text{-P}_s$	675.61	0.3243			
$\text{P}_s\text{-P}_s$	52 905.81	0.2795			
$\text{P}_s\text{-P}_s\text{-P}_s$			1241.15		
$\text{Ge}_c\text{-P}_s\text{-P}_s$			-99.37		
$\text{Zn}_c\text{-P}_s\text{-P}_s$			-258.9		
$\text{P}_c\text{-P}_s$				-1.674	1.01

TABLE II. Calculated and experimental bulk properties of ZnGeP₂.

Property	Calculated	Experimental
Lattice constants, Å		
<i>a</i>	5.462	5.467 ^a
<i>c</i>	10.717	10.715 ^a
<i>c/a</i>	1.962	1.958
Elastic constants, dyn cm ⁻²		
<i>C</i> ₁₁	8.32	8.7 ^b
<i>C</i> ₁₂	4.47	6.6 ^b
<i>C</i> ₁₃	4.91	6.4 ^b
<i>C</i> ₃₃	8.34	8.1 ^b
<i>C</i> ₄₄	3.50	2.9 ^b
<i>C</i> ₆₆	3.23	2.8 ^b
Dielectric constants		
ε ₀ ¹¹	10.89	11.21 ^c
ε ₀ ³³	12.15	11.40 ^c
ε _∞ ¹¹	9.44	9.75 ^c
ε _∞ ³³	9.89	9.91 ^c

^aReference 19.

^bValues from lattice dynamics calculations (Ref. 24).

^cReference 20.

roduces the change in defect energies less than 0.03 eV showing a satisfactory accuracy of our results. Note that given an adequate interatomic potential description of the lattice, these calculations have been proven to provide reliable values of defect energetics.¹⁷

The calculated Schottky, Frenkel, and antisite formation energies (per defect) are listed in Table III. In ZnGeP₂, the Schottky defect is (V_{Zn}+V_{Ge}+2V_P), the Frenkel defect pairs are (V_{Zn}+Zn_i), (V_{Ge}+Ge_i) and (V_P+P_i), and the antisite pair in the cation sublattice is (Zn_{Ge}+Ge_{Zn}). As shown, the lowest formation energy comes out to be for (Zn_{Ge}+Ge_{Zn}) antisite pair. The magnitude of this energy is small (0.25 eV) suggesting that appreciable disorder would occur in the cation sublattice at higher temperatures. These antisite defects are then followed by the Frenkel pairs of Zn and Ge. For the Schottky defect, the large formation energies would seem to preclude its existence as intrinsic point defects in the lattice.

Experimentally, electronic defects including both electron and hole centers in as-grown ZnGeP₂ have been identified by the magnetic resonance studies. An EPR spectrum associated with a hole center was first observed by Kiel²⁶ who suggested the center to be P₂⁵⁻, analogous to the V_k center in halides. Recently, Rakowsky *et al.* have performed a detailed study of the angular dependence of the EPR spec-

TABLE III. Formation energies (per defect) in ZnGeP₂.

Defect	Formation energy (eV)
Antisite (Zn _{Ge} +Ge _{Zn})	0.13
Frenkel	
Zn	1.1
Ge	2.2
P	4.7
Schottky	8.7

TABLE IV. Binding energies of electronic defects in ZnGeP₂. (The positive values indicate the stability of the defect complexes in the lattice.)

Defect	Binding energy (eV)
Hole near V _{Zn}	
1-center	0.57
2-center	0.35
4-center	0.12
Hole near Zn _{Ge}	
1-center	-0.01
2-center	-0.08
4-center	0.17
Hole near V _{Ge}	
1-center	0.20
2-center	-0.18
4-center	-0.35
Electron near V _P	
2-center	0.68

trum suggesting that either a zinc vacancy or a zinc ion on a germanium site forms the acceptor center. Their hyperfine analysis indicates that the hole is equally shared between two near-neighbor phosphorus ions.¹¹ A recent ENDOR study favors the singly ionized zinc-vacancy model based on the requirement of a large lattice distortion near the defect complex.¹² It was suggested that the observed change in the angle between the interphosphorus axis and the basal plane of the crystal can only be due to the presence of the zinc vacancy.

For calculations, we follow a similar approach proposed first for tetrahedrally coordinated semiconductor, ZnSe.¹⁶ Our aim is to obtain binding energy and lattice distortion in both the possibilities for the acceptor center, i.e., a hole may be trapped near a zinc vacancy forming a center similar to the V⁻ center in oxides²⁷ or may be localized in the vicinity of an antisite defect, Zn_{Ge}. The binding energy of a hole to a defect will then be

$$E_{\text{binding}} = E_{h+D} - E_h - E_D, \quad (3)$$

where *D* is either V_{Zn} or Zn_{Ge} and *E*_{*h+D*} refers to the total energy of the defect complex.

In these calculations, we consider the cases where either the hole is localized near only one of the near-neighbor P atoms (i.e., 1-center case) or the hole is shared by a pair of near-neighbor P atoms (i.e., 2-center case) or the hole is distributed over the near-neighbor P atoms (i.e., 4-center case). We assume that the trapping of a hole only changes long-range Coulombic interactions. Short-range interactions between P ions sharing the hole and the surrounding ions are taken to be that of the perfect lattice. For the 2- and 4-center cases, the equal sharing of the hole by two and four neighboring P atoms reduces the shell charge of the corresponding P atoms by (1/2)*e* and (1/4)*e*, respectively.

Table IV lists the calculated binding energies of the hole centers in ZnGeP₂. The binding energy of a hole equally shared by two near-neighbor P ions (i.e., 2-center case) comes out to be much larger in the vicinity of the Zn vacancy than that of the Zn_{Ge} site. This clearly demonstrates that the

$(h2 + V_{Zn})$ defect complex is relatively more stable in the lattice. In comparing the binding energies for different hole localization regions in both the Zn vacancy and antisite cases we can see a striking distinction. The hole tends to be localized near a Zn vacancy, i.e., the more the hole is localized, the larger the binding energy but the trend is exactly opposite for the antisite defect and a hole cannot be localized near the Zn_{Ge} site. Thus, the acceptor center can only be stabilized by the Zn vacancy in the lattice. This conclusion is also supported by the defect geometry considerations in the lattice. For $(h2 + V_{Zn})$, the nearest-neighbor P ions relax significantly (12% of a bond length) towards the vacancy, whereas only a small relaxation (2% of a bond length) occurs for these ions for the $(h2 + Zn_{Ge})$ defect complex. The results therefore show that the association of the zinc vacancy introduces a very large distortion in the lattice corroborating the analysis of the ENDOR spectrum. We also note here that the acceptor binding energy comes out to be 0.57 eV as compared to the experimental value of 0.5–0.55 eV usually obtained from temperature dependence of the Hall effect or of the resistivity.^{7,28} On the other hand, analysis of IR absorption spectra generally gives a value in the range of 0.6–0.7 eV.²⁹

For the acceptor center associated with the Ge vacancy, the calculations predict binding for the hole only in the 1-center case. For the 2- and 4-center cases, the defect complex is not stable (Table IV). There is no experimental observation that the V_{Ge} defect complex whose stability we calculate exists. The literature just does not address the possibility that two native acceptors exist. However, it is possible to reinterpret past data in light of this result. If the V_{Ge} defect is well compensated, then Hall effect data would reveal only the deeper V_{Zn} defect. On the other hand, if the V_{Ge} defect is only partially compensated, the Hall data would reveal its activation energy, or in the special case, that the defect is nearly exactly compensated, the apparent activation energy from a two level acceptor–donor analysis would be the average of the deeper and shallower energy. Using the energies in Table IV as an example, one could expect to see a range of Hall activation energies (i.e., 0.2, 0.35, and 0.57 eV) due to changes in the compensation level.

Sodeika *et al.*⁸ have reviewed the Hall activation energies ranging from 0.3 to 0.57 eV in $ZnGeP_2$. Using a two level model, they have attributed this variation to interactions with a nearby compensated donor at high compensation levels which has the effect of moving the isolated activation energy from the deeper value to the shallower value. In a three level model such a change in the Hall activation energy can be explained by varying the compensation ratio of the shallower acceptor from less than one to greater than one. Very clear examples of shallow Hall activation energies ranging from 0.31, 0.33, and 0.35 eV are referenced.⁸ This could be interpreted using a three level model as a case where the partially compensated shallow V_{Ge} defect activation energy of 0.31–0.35 eV is being observed directly. When it is overcompensated the activation energy of 0.50–0.57 eV of the V_{Zn} defect is observed. Past photoluminescence studies of $ZnGeP_2$ may also have revealed the V_{Ge} defect as compensated centers. For example, in a massive

study of over 100 samples grown in different ways and variously doped Averkieva *et al.*³⁰ report that luminescence is generally seen at ~ 1.6 and 1.3 eV attributed to two levels located 0.49 and 0.79 eV from a band edge. In a three level model, we suggest that the 1.6 eV recombination energy could be attributed to the V_{Ge} defect and 1.3 eV to the V_{Zn} defect. Therefore, the reported Hall effect and photoluminescence data are compatible with a three level model (i.e., two acceptors and one donor) where one of the acceptors is significantly shallower, experimentally by 0.27 eV, in reasonable agreement with the calculated difference of 0.37 eV.

While the zinc vacancy is the dominant acceptor in $ZnGeP_2$, the phosphorus vacancy (V_P^0) is found to be the dominant donor in the as-grown material that is associated with a photoinduced EPR center in the lattice.¹³ The proposed model for this EPR center suggests that two zinc ions neighboring the phosphorus vacancy unequally share an unpaired spin. At present, electron density distribution calculations are beyond the limitations of this atomistic shell model. However, we can calculate the binding energy of the defect complex assuming an equal sharing of the electron by two zinc atoms near the P vacancy. The binding energy turns out to be about 0.68 eV showing that the EPR center is very stable in the lattice.

Cation disorder in $ZnGeP_2$ is a subject of much controversy. The phase diagram obtained by differential thermal analysis (DTA) shows a phase transition from a random (cation) zinc-blende phase to an ordered (cation) chalcopyrite phase upon cooling through 950 °C.¹ However, recent experimental studies do not provide direct evidence for the phase transition. For example, electrical resistance measurements taken from room temperature to the melting point showed no evidence of the phase transition.³¹ On the other hand, anomalous small sidebands observed in Raman spectra were initially interpreted as a direct observation of lattice disorder.²⁰ More recently, it has been shown that the disorder is limited to the near-surface region as spectroscopy using more penetrating wavelengths, shows no evidence of disorder.³² Finally, a theoretical study³³ on the phase stability of $ZnGeP_2$ shows that the zinc-blende phase is energetically unfavorable as compared to all of the possible ordered phases (including chalcopyrite, Cu–Au, Cu–Pt, and Z2 phases). Considering the small defect formation energy associated with antisites that we have calculated and the lack of evidence for the zinc-blende phase in $ZnGeP_2$ yields an interesting paradox.

IV. SUMMARY

The work described here has demonstrated that $ZnGeP_2$ can be simulated successfully in the framework of the shell model with fractional charges for the constituting ions in the lattice. The lattice and dielectric constants are well-described by this potential model.

The calculated defect energies and lattice distortion corroborates the ENDOR spectrum associating the zinc vacancy with the acceptor center in $ZnGeP_2$ and the calculated binding energies for it are in agreement with values reported from absorption and Hall effect measurements. The binding en-

ergy of the P vacancy donor has been found to be deep as anticipated and its value of 0.68 eV is reported here.

On the other hand, cation sublattice disorder in the form of antisite defect pairs is predicted to be the dominant native defect on the basis of formation energies. If antisites are present in large concentration their behavior must be quite benign. From our calculations, a hole cannot bind to a Zn antisite therefore, this defect cannot behave as an acceptor as generally expected.¹¹ If there is a similar inability to bind a charge carrier to the Ge antisite, then antisites even if present in large numbers will not play a dominant role in determining the properties of the material.

There is no direct evidence that the Ge vacancy acceptor defect whose properties we calculated exists. However, reported Hall effect and photoluminescence data are shown to be compatible with the existence of two acceptors where one is significantly shallower, experimentally by 0.27 eV, in reasonable agreement with calculated difference of 0.37 eV. Furthermore, we note here that the observed cation vacancy defect corresponds to the cation with the larger ionic radius. In diamondlike semiconductors, vacancies of large cations are generated to minimize strain. Examples are HgCdTe, CuInSe₂, CuInS₂, CdGeAs₂, and CdSiP₂ and ZnGeP₂.

The dominant defects controlling the properties of the material would seem to be the Zn vacancy with a binding energy of 0.57 eV which is partially compensated by a P donor vacancy which has a binding energy of 0.68 eV. However, a three level model which includes the shallower Ge vacancy acceptor defect which is usually overcompensated cannot be ruled out.

ACKNOWLEDGMENTS

The authors wish to acknowledge helpful discussions with Dr. Marge Rakowski and Captain Walt Lauderdale. This research was sponsored by the U.S. Air Force under Contract No. AFOSR-F49620-94-1-0228.

¹J. L. Shay and J. H. Wernick, *Ternary Chalcopyrite Semiconductors: Growth, Electronic Properties and Applications* (Pergamon, Oxford, 1974).

²G. C. Bhar, Jpn. J. Appl. Phys. **32**, 653 (1993).

³E. K. Gorton, P. D. Mason, and D. J. Jackson, Opt. Commun. **110**, 163 (1994).

⁴P. A. Budni, K. Ezzo, P. G. Schunemann, S. Minnigh, J. C. McCarthy, and T. M. Pollak, edited by G. Dube and L. L. Chase, *OSA Proceedings on Advanced Solid State Lasers* (Optical Society of America, Washington, DC, 1991), Vol. 10, p. 335.

⁵P. G. Schunemann, P. A. Budni, M. G. Knights, T. M. Pollak, E. P. Chicklis, and C. L. Marquardt, *Advanced Solid State Lasers and Compact Blue-Green Laser Technical Digest* (Optical Society of America, Washington, DC, 1993), Vol. 2, p. 131.

⁶Yu. V. Rud, Fiz. Techn. Poluprovodn. **28**, 633 (1994).

⁷G. Balcaitis, Z. Januskevicius, and A. Sodeika, Phys. Status Solidi A **89**, K71 (1985).

⁸A. Sodeika, Z. Silvevicius, Z. Januskevicius, and A. Sakakas, Phys. Status Solidi A **69**, 491 (1982).

⁹V. N. Brudnyi, D. L. Budnitskii, M. A. Krivov, R. M. Masagutova, V. D. Prochukhan, and Yu. V. Rud, Phys. Status Solidi A **50**, 379 (1978).

¹⁰V. N. Brudnyi, V. A. Novikov, A. D. Pogrebnyak, and Yu. P. Surov, Phys. Status Solidi A **83**, K35 (1984).

¹¹M. H. Rakowsky, W. K. Kuhn, W. J. Lauderdale, L. E. Halliburton, G. J. Edwards, M. P. Scripsick, P. G. Shunemann, T. M. Pollak, M. C. Ohmer, and F. K. Hopkins, Appl. Phys. Lett. **64**, 1615 (1994).

¹²L. E. Halliburton, G. J. Edwards, M. P. Scripsick, M. H. Rakowsky, P. G. Shunemann, and T. M. Pollak, Appl. Phys. Lett. **66**, 2670 (1995).

¹³N. C. Giles, L. E. Halliburton, P. G. Shunemann, and T. M. Pollak, Appl. Phys. Lett. **66**, 1758 (1995).

¹⁴J. E. Jaffe and A. Zunger, Phys. Rev. B **30**, 741 (1984).

¹⁵V. G. Tyuterev, Fiz. Tverd. Tela **31**, 1428 (1989).

¹⁶J. H. Harding and A. M. Stoneham, J. Phys. C: Solid State Phys. **15**, 4649 (1982).

¹⁷*Computer Simulation of Solids*, edited by C. R. A. Catlow and W. C. Mackrodt (Springer, Berlin, 1982).

¹⁸B. G. Dick and A. W. Overhauser, Phys. Rev. **112**, 90 (1958).

¹⁹J. D. Wolf (private communication).

²⁰F. Lu and C. H. Perry, Bull. Am. Phys. Soc. **36**, 1014 (1991).

²¹J. D. Gale, Philos. Mag. B (in press).

²²J. D. Gale, General Utility Lattice Program, developed at the Royal Institution of Great Britain/Imperial College, 1992.

²³B. M. Axilrod and E. Teller, J. Chem. Phys. **11**, 299 (1943).

²⁴A. S. Poplavnoi, Izv. Vyssh. Uchebn. Zaved. Fiz. **8**, 5 (1986).

²⁵A. B. Lidiard and M. J. Norgett, in *Computational Solid State Physics*, edited by F. Herman (Plenum, New York, 1972), p. 385.

²⁶A. Kiel, Solid State Commun. **15**, 1021 (1974).

²⁷J. H. Harding, J. Phys. C: Solid State Phys. **12**, 3931 (1979).

²⁸V. Yu. Rud and Yu. V. Rud, Jpn. J. Appl. Phys. **32**, Suppl 32-3, 672 (1993).

²⁹H. M. Hobgood *et al.*, J. Appl. Phys. **73**, 403 (1993).

³⁰G. K. Averkieva, V. S. Grigoreva, I. A. Maltseva, V. D. Prochukhan, and Yu. V. Rud, Phys. Status Solidi A **39**, 453 (1977).

³¹P. G. Schunemann (private communication).

³²S. Tlali, H. E. Jackson, M. C. Ohmer, P. G. Schunemann, and T. M. Pollak, Bull. Am. Phys. Soc. **40**, 760 (1995).

³³R. McCormack and D. Fontaine (private communication).